Union of Mathematicians of Macedonia - ARMAGANKA

IX SEMINAR OF DIFFERENTIAL EQUATIONS AND ANALYSIS

and

1st CONGRESS OF DIFFERENTIAL EQUATIONS, MATHEMATICAL ANALYSIS AND APPLICATIONS

CODEMA 2020

Proceedings of the CODEMA 2020
Зборник на трудови од CODEMA 2020

Skopje, 2021

DETERMINATION OF THE GEOMETRIC (*m*,*n*) STRUCTURE OF EXPERIMENTALLY PRODUCED CNTs

ISBN 978-608-4904-09-0 UDC:514.123:546.24-022.532]:004.92

Viktor Andonovic, Aleksandar T. Dimitrov,Perica Paunovic, Beti Andonovic

Abstract. Each carbon nanotube (CNT) has its own mathematical representation due to its hexagonal lattice structure. The subjects of research are multi-wall carbon nanotubes (MWCNTs) and determining their structural parameters: innermost and outermost diameters, chiral indices *m* and *n*, number of walls and their unit cell parameters. Within this paper low frequency region and corresponding high frequency parts of Raman spectra of three experimentally produced CNTs are considered, as well as Python programming for the most accurate (*m*,*n*) assignment. Determining the chirality of these samples enables calculation of other structural properties which are performed hereby. Furthermore, this author's work enables future studies on the samples, as are calculation of different topological indices using the graph representation and the chirality of the studied CNT samples.

1. INTRODUCTION

Carbon nanotubes (CNTs) are allotropes of carbon in nanodimensions with highly outstanding properties. Since graphene is a 2D building unit of all carbon allotropes, such as fullerenes, CNTs, nanoribbons, and so on, CNTs may be observed as wrapped up graphene structure having an ideal cylindrical shape, as shown in Fig. 1 A, B [4].

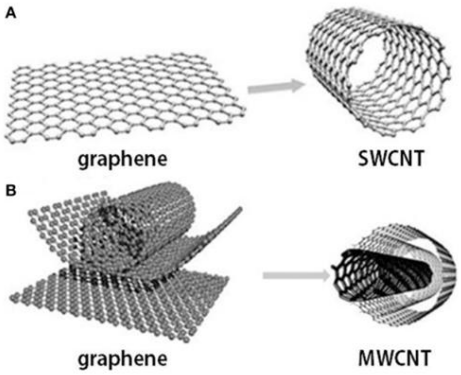

Figure 1: Graphene sheet as a 2D building unit of A) SWCNT; B) MWCNT.

2010 *Mathematics Subject Classification.* Primary: 51N20 Euclidean analytic geometry, 92E10 Molecular structure Secondary: 68-04 Computer science.
Key words and phrases. chiral indices, CNTs' structure, MWCNT, Python

Each nanotube has its own mathematical representation due to its hexagonal lattice structure [1],[2]. The geometric structure analysis of carbon nanotubes has been quite a challenging task, particularly if the subject of research is multi-wall carbon nanotubes (MWCNTs) [1]-[3], [5]-[8]. Knowing CNTs structural parameters (diameter, chiral angle, chiral indices m and n) is basically knowing their properties, which is essential for any research in the field of CNTs and their application. There are several excellent tools as are HRTEM, ED, RRS and others that suggest some models of (*m,n*) assignment for single-wall carbon nanotubes (SWCNTs), as well as for MWCNTs. However, precise determination of the CNTs atomic structure features becomes extremely complicated for more than three walls (layers) [5]. Thorough and overall analyses and use of experimental results combined with recent theoretical background may lead to successful estimation of its structural elements.

Within this paper Raman spectra of three experimentally produced CNTs of undetermined diameter, chirality, and number of walls, are considered, having assigned nomenclatures: CNT_1, CNT_2, and CNT_3. Due to the fact that their properties are tightly connected and dependent on their atomic structure, detailed analyses with regard to determining their diameters, calculating their chiral indices *m* and *n*, and furthermore other parameters, were calculated, hence estimating the number of walls (layers) of each nanotube. This research was strictly focused to determination of outermost and innermost diameters, as well as corresponding chiral indices, estimation of the number of other inner diameters, which would implicate the number and the nature of CNT's walls. Knowing the chirality of these samples enables calculation of other structural properties which are performed hereby. Authors strongly suggest future studies on the samples, as are performing additional EDP analysis to enhance and confirm the accuracy of applied methods, as well as calculation of different topological indices using the graph representation and the chirality of the studied samples, since it is known that they are related to some properties of the corresponding molecules.

2. MATERIALS AND TECHNIQUES

The carbonaceous phases extracted from the solidified electrolyte were observed by scanning electron microscopy, using JEOL 6340F (SEM, 10 kV). Structural characteristics of the carbon nanostructures were studied by means of Raman spectroscopy. Non-polarized Raman spectra were recorded by a confocal Raman spectrometer (Lab Ram ARAMIS, Horiba Jobin Yvon) operating with a laser excitation source emitting at 532 nm. The low frequency regions 50-350 cm^{-1} were taken into consideration, as well as the frequency regions 1200-1800 cm^{-1} from the Raman spectra of the CNTs. Python programming was applied to determine possible chiral indices assignment to the studied samples.

3. ANALYSES AND APPROACHES TO THE CNT SAMPLES

Knowing the mathematical representation of CNTs, due to its hexagonal lattice atomic structure, one can determine the relations among various CNT parameters: unit vectors $\vec{a}_1$ and $\vec{a}_2$, chiral vector $\vec{C}_h$, CNT diameter d_{CNT}, chiral angle θ, translation vector $\vec{T}$ of the CNT unit cell (being the shortest repeat distance along the nanotube axis), number of hexagons N_H, number of vertices (atoms) and so on, (Fig. 2), which are expressed with the formulas (1)-(5). Lattice constants are the lengths of the unit vectors $a = |\vec{a}_1| = |\vec{a}_2| = 0.246$ nm and the distances between neighbouring carbon atoms are $a_{C-C} = 0.142$ nm [1].

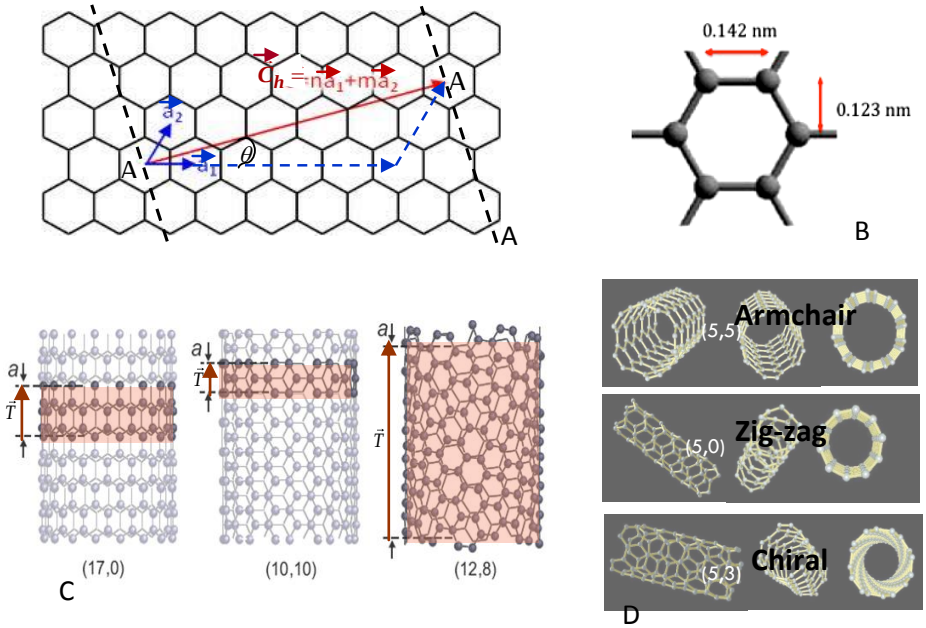

Figure 2: A) Atomic mathematical CNT structure; B) CNT constants; C) Various CNT unit cells; D)Three CNT types according to θ.

$$\left|\vec{C}_h\right| = \sqrt{3}a_{C-C}(m^2 + mn + n^2)^{1/2} \text{ nm} \qquad (1)$$

$$d_{CNT} = \frac{\sqrt{3}a_{C-C}(m^2 + mn + n^2)^{1/2}}{\pi} = 0.079\sqrt{(m^2 + mn + n^2)} \text{ nm} \qquad (2)$$

$$\theta = arctg\frac{\sqrt{3}n}{2m+n}, \quad 0 \le \theta \le \frac{\pi}{6} \quad (0 \le n \le m) \qquad (3)$$

$$\theta = \frac{\pi}{6} \quad -\text{armchair CNT}, \quad \theta = 0 \quad -\text{zig-zag CNT}, \quad 0 < \theta < \frac{\pi}{6} \quad -\text{chiral CNT}$$

$$T = \left|\vec{T}\right| = \frac{\sqrt{3}\left|\vec{C}_h\right|}{d_R} = \frac{\sqrt{3}\pi d_{CNT}}{d_R} \text{ nm}, \tag{4}$$

$d_R = GCD(2m+n, 2n+m)$, given by

$$d_R = \begin{cases} d, & \text{if } m-n \text{ is not a multiple of } 3d \\ 3d, & \text{if } m-n \text{ is a multiple of } 3d \end{cases}$$

where $d = \text{GCD}(m,n)$

$$N_{\text{H}} = \frac{2(m^2+mn+n^2)}{d_R} \tag{5}$$

There are different experimental methods of producing CNTs, and based of the procedure, they can be either SWCNTs or MWCNTs. The CNT with the lowest reported diameter value experimentally produced is known to have the diameter $d_k = 4\text{Å}$ [10]. As theoretically predicted, it is the narrowest attainable that can still remain energetically stable. Such nanotubes may be the innermost constituent layer of MWCNTs. In contrast to CNTs with larger diameters, whose conductivity nature depends on their diameter and helicity (chirality), these smallest nanotubes are always metallic, regardless of the chirality [10]. For every other CNT it holds that it is metallic, if and only if it satisfies the condition $\text{MOD}(2m+n,3)=0$. In Fig. 3 images of experimentally obtained MWCNT samples at the Faculty of Technology and Metallurgy in Skopje are presented.

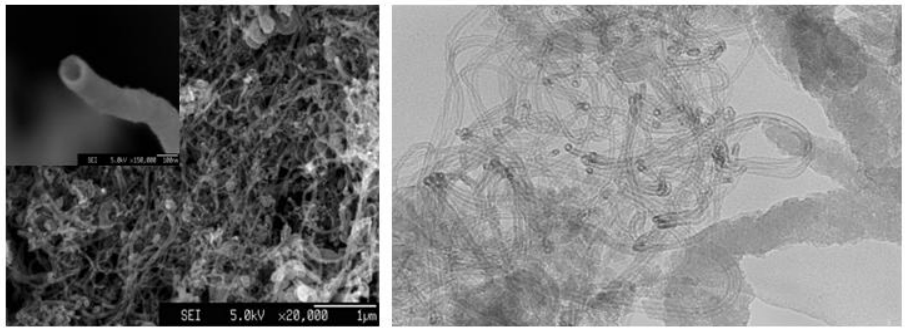

Figure 3: SEM and TEM images of experimentally obtained MWCNT

To date, the atomic geometric structure of carbon nanotubes determination and analysis has been quite a challenging task, particularly if the subject of research is MWCNTs. Three CNTs, experimentally produced, are considered for analyses in this research: CNT_1, CNT_2, and CNT_3. Each of the three nanotubes is undetermined with regard to its diameter, chirality and number of walls. The focus of this research is strictly focused to determination of their diameters, both

innermost and outermost diameters denoted by d_i and d_o correspondingly, determination of chiral indices (*m*,*n*), the total number and nature of other inner walls (layers), each having a diameter d_k, and the interlayer distance δ_r^k (Fig. 4). The latter are known to usually be within the interval $0.32\,\text{nm} \le \delta_r^k \le 0.35\,\text{nm}$, although it can sometimes vary from $0.27\,\text{nm}$ up to $0.35\,\text{nm}$ [9].

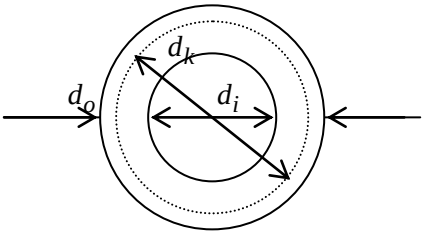

Figure 4: Diameters of MWCNTs

The relation among the diameters and the interlayer distances (Fig. 4) is given by

$$\delta_r^k = \frac{d_k - d_{k-1}}{2},$$

whereas by

$$N = \frac{d_o - d_i}{2\delta_r} + 1$$

the relation among the number of layers *N*, the innermost diameter d_i, the outermost diameter d_o, and the average interlayer distance δ_r is given.

The key role within our analyses was assigned to the Raman spectra in two frequency regions of each nanotube samples: $\omega \in [50\,\text{cm}^{-1}, 350\,\text{cm}^{-1}]$ and $\omega \in [1200\,\text{cm}^{-1}, 1800\,\text{cm}^{-1}]$. The first region was expected to point to the Radial breathing mode (RBM) frequencies at SWCNTs, and to Radial breathing-like mode frequencies (RBLM) at MWCNTs. These measurements can be used as an accurate tool to estimate the diameters of each layer of the tubes, since RBM is an active mode where all carbon atoms move in-phase in the radial direction. Several experimental relations have been established between the diameter of the tube and the RBM frequency ω_{RBM} [5]. Within a limited range of diameters, those relations are equivalent. While (6) is more accurate when small diameters are considered, (7) is more useful when it comes to very large diameters (or extremely low frequencies). The dependence of the innermost diameter d_i and the outermost diameter d_o on the corresponding frequency is given by the established relations in (6), whereas relation (7) can be used for much larger range of diameters, and whenever relation (6) is unusable or unreliable, due to the size of the outermost diameter. One may notice that d_i is obtained by the same equation as d_o, with C_e being 0. The latter is due to the fact that the parameter C_e is conventionally used to express different environmental conditions around the nanotube. The innermost concentric nanotube within the MWCNT is not affected by such conditions, which is not the case with the outermost concentric tube.

$$d_i = \frac{228}{\omega_i^{RBLM}}$$

$$d_o = \frac{228}{\sqrt{(\omega_o^{RBLM})^2 - 228^2 \cdot C_e}}, \qquad C_e = 0.065\,\mathrm{nm}^{-2} \tag{6}$$

$$\omega_{RBM} = \frac{A}{d} + B \tag{7}$$

$$A = 223\,\mathrm{cm}^{-1}, \quad B = 10\,\mathrm{cm}^{-1}$$

Another frequency region to help the analysis is the high frequency region of G-modes, showing off in the interval $\omega \in (1500\,\mathrm{cm}^{-1}, 1600\,\mathrm{cm}^{-1})$. A useful diameter dependence for the chiral CNTs (semiconducting or metallic), which was used as a control method herein, is given by the formulas (8) and (9) [5].

$$\omega_{TO}^{G}(d) = 1582 - \frac{27.5}{d^2}, \quad \text{for semiconducting chiral} \tag{8}$$

$$\omega_{LO}^{G}(d) = 1582 - \frac{38.8}{d^2}, \quad \text{for metallic chiral} \tag{9}$$

The number of components in the G-peak is an excellent indicator of the conductive nature of the studied CNT sample [5]. Table 1 will help the analysis when the chiral indices assignment to the samples is done.

Table 1: Dependence between G-peak components and the CNT conductivity

Nanotube	**Number of components**	**G-peak profile**
Semiconducting chiral (SC)	2	LO, TO: narrow, symmetric
Metallic chiral (MC)	2	LO: broad, asymmetric TO: narrow, symmetric
Armchair	1	TO: narrow, symmetric
Semiconducting zigzag (SZ)	1	LO: narrow, symmetric
Metallic zigzag (MZ)	1	LO: broad, symmetric

3. RESULTS AND DISCUSSIONS

3.1. NANOTUBE CNT_1. (n,m) ASSIGNMENT RESULTS

The Raman spectra in both frequency regions for CNT_1 are shown in Fig. 5 A, B. There is only one peak in the low frequency region, which indicates that the nanotube is a single-wall, i.e. $d^{(1)} = d_o^{(1)}$. Using (6), it is obtained:

$$d^{(1)} = d_o^{(1)} = 0.665\,\mathrm{nm}$$

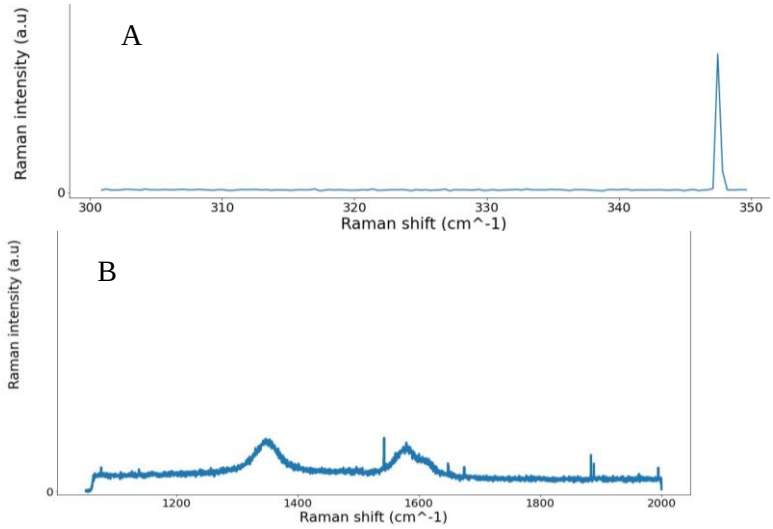

Figure 5: A) Raman spectrum RBM mode for CNT_1;
B) Raman spectrum G-mode for CNT_1

The determined diameter is lower than 1 nm and the most accurate results are expected for diameters 1 nm – 2.5 nm, hence the interval for calculating possible chiral indices candidates was performed within somewhat broader diameter interval $(d^{(1)} - 0.02, d^{(1)} + 0.02)$. Python programming was applied for obtaining possible candidates to satisfy equation (2), and the results of 24 possibilities are indicated in Table 2.

Table 2: Possible (*m*,*n*) assignments for diameter $d^{(1)} = 0.665\,\text{nm}$ of CNT_1

(4,3)	(4,4)	(5,2)	(5,3)	(5,4)	(5,5)
(6,0)	(6,1)	(6,2)	(6,3)	(6,4)	(6,5)
(6,6)	(7,0)	(7,1)	(7,2)	(7,3)	(7,4)
(7,5)	(8,0)	(8,1)	(8,2)	(8,3)	(8,4)

Due to the broadness of the G-peak (see Fig. 5 B), the chiral indices candidate pairs need to satisfy the metallic condition $\text{MOD}(2m+n,3)=0$. Hence, only the five chiral indices pairs in red (see Table 2) are considered. However, the armchair type (5,5) would show one narrow and symmetric G-peak, and the chiral metallic (6,3), (7,1), and (8,2) would show two components of the G-peak, one being narrow (see Table 1), which here is not the case.

This leaves only one possibility, the zig-zag metallic tube (6,0), which is in high accordance with the broad and asymmetric G-peak of the nanotube CNT_1.

In Figure 6 there is an illustration of CNT_1 with determined diameter and chiral indices assignment.

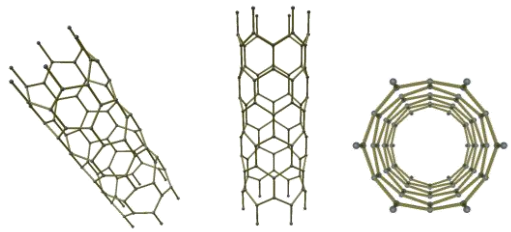

Figure 6: Visual model of (6,0) SWCNT

3.2. NANOTUBE CNT_2. (n,m) ASSIGNMENT RESULTS

The Raman spectra in PBLM frequency region, as well as in G-mode region for CNT_2 are shown in Fig. 7 A, B. There are two peaks in the low frequency range, which identifies the CNT_2 as double-wall CNT (DWCNT).

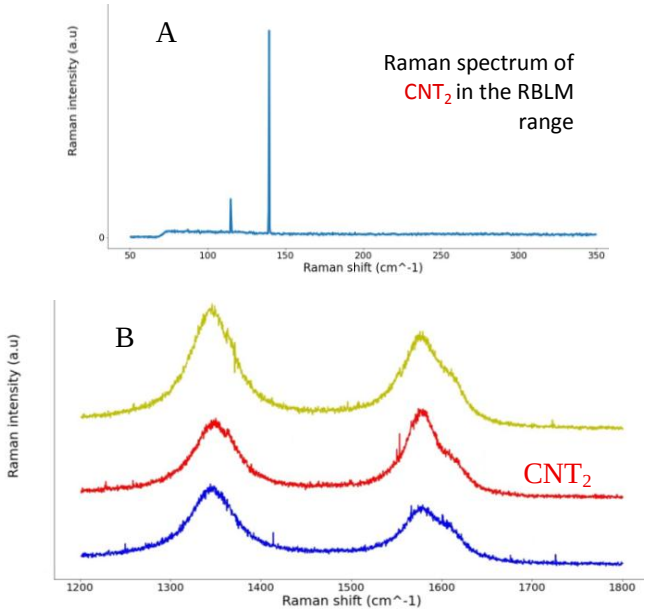

Figure 7: A) Raman spectrum RBLM modes for CNT_2;
B) Raman spectrum G-mode range for CNT_2

According to the corresponding frequency values in Fig.7 A and equation (6), both the innermost and outermost diameters are calculated as follows.

$d_i^{(2)} = 1.63\,\text{nm}$

$d_o^{(2)} = 2.3\,\text{nm}$

The interlayer distance is calculated as $\delta_r = \frac{d_o - d_i}{2} = 0.335\,\text{nm}$, which is the equilibrium distance for tubes that are DWCNTs [5].

Considering the G-mode range, and depending on the chiral or achiral character of each constituent SWNT, one expects to observe 4 (chiral@chiral), 3 (chiral@achiral or achiral@chiral) or 2 (achiral@achiral) components in the Raman spectrum measured on an individual DWNT. However, some components can appear at close frequencies and thus cannot be experimentally resolved. Consequently, the number of observed components can be less than the one predicted or expected for different configurations (see Table 1). With regard to CNT_2, two identified components of the G-peak are located at the frequencies 1570.98 cm^{-1} and 1574 cm^{-1}. These frequencies enable the estimating of the diameters, and hence it is obtained $d_i^{(2)} = 1.58\,\text{nm}$ by using equation (8), which implicates a semiconducting chiral layer, and $d_o^{(2)} = 2.25\,\text{nm}$ by using equation (9), which implicates a metallic chiral layer. One may notice that the obtained diameters by both methods are in high accordance, and the values obtained by (6) are kept as accurate.

The determined diameters are within 1 nm – 2.5 nm, hence the interval for calculating possible chiral indices candidates was performed within narrower diameter interval with a 0.01 nm error bar $(d^{(2)} - 0.01, d^{(2)} + 0.01)$. Python programming was applied for obtaining possible assignment candidates for both diameters to satisfy equation (2), and the results of 16 combinations are derived from the pairs indicated in Table 3.

Table 3: Possible (*m*,*n*) assignments for the innermost and outermost diameters of CNT_2

$d_o^{(2)}$	$d_i^{(2)}$
(22,11)	(12,12)
(25,7)	(13,11)
(27,4)	(17,6)
(28,2)	(19,3)

Qualitative analysis of the G-peak indicated a broad component, hence a metallic chiral character of one layer and semiconducting chiral character of the other layer. Hence, the possible cases are either MC@SC or SC@MC, which corresponds to the implications from equations (8) and (9) results. The only chiral indices pair assignment satisfying the MC condition is (25,7). There are three possibilities of type SC@MC: (13,11)@(25,7), (17,6)@(25,7), and (19,3)@(25,7). The exact innermost and outermost diameters of these three possibilities give interlayer distances 0.329 nm, 0.335 nm, and 0,335 nm correspondingly. The latter eliminates the first tube, and, the remaining two possibilities (17,6)@(25,7), and (19,3)@(25,7) are equally possible up to here. However, it is possible to make a strong distinction between these two

possibilities by an additional method of performing and analyzing an EDP of the CNT_2. Authors suggest such further research, since this analysis would estimate the ratio *m*/*n*, which greatly differs at the last two possibilities. It is highly expected that it would leave only one candidate combination.

In Fig. 8 there is an illustration of the two candidates with determined diameters and chiral indices assignment to the tube CNT_2.

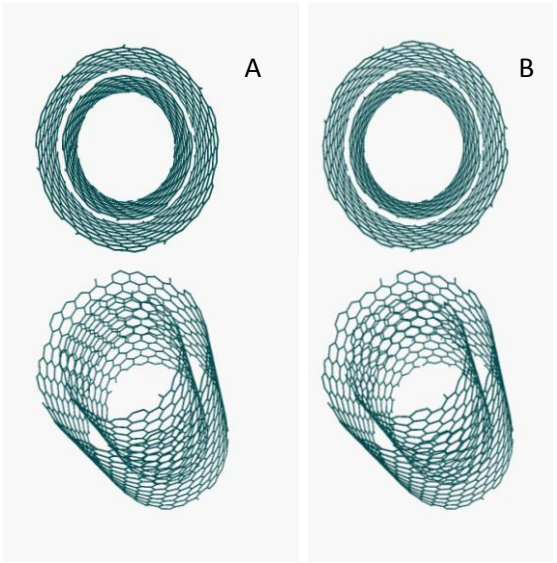

Figure 8: Visual model of A) (17,6)@(25,7); B) (19,3)@(25,7)

3.3. NANOTUBE CNT_3. (n,m) ASSIGNMENT RESULTS

Several (six) peaks may be noticed in the Raman spectra in PBLM frequency region of CNT_3 (Fig. 9 A), which identifies this nanotube as MWCNT. Presence of both narrow and broad components in the G-mode range (Fig. 9 B) implicates both semiconducting and metallic layer in the structure of CNT_3. According to the corresponding frequency values in Fig.9 A and equation (6), both the innermost and outermost diameters are calculated as follows:

$$d_i^{(3)} = 0.65\,\text{nm}$$

$$d_o^{(3)} = 7.73\,\text{nm}$$

The frequency of the outermost diameter $d_o^{(3)}$ is extremely low and near the limit of possible calculation, therefore its calculation may have a high error bar or even be highly inaccurate. Hence, the outermost diameter is recalculated using equation (7) and following result is obtained:

$$d_o^{(3)} = 4.04\,\text{nm}$$

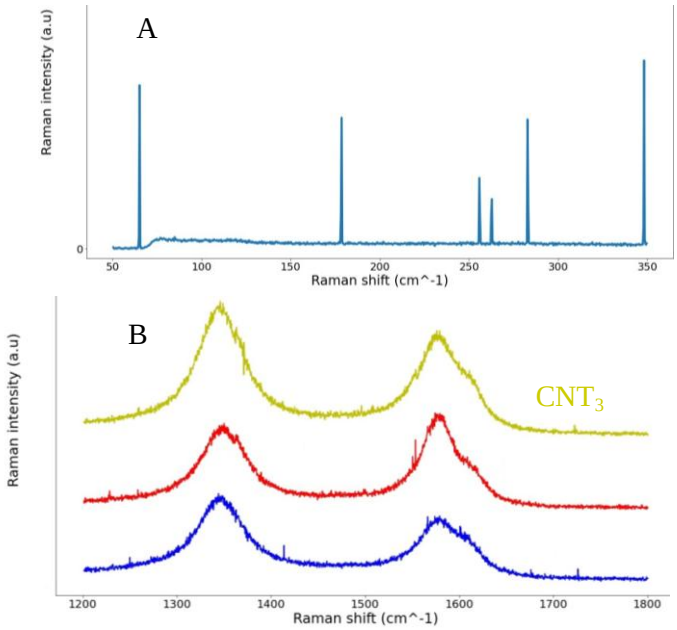

Figure 9: A) Raman spectrum RBLM modes for CNT_3;
B) Raman spectrum G-mode range for CNT_3

To be able to decide which outermost diameter value is good, equation (8) is applied for the G-peak component frequency $\omega = 1580.34\,\mathrm{cm}^{-1}$. Thus it is obtained $d_o^{(3)} = 4.07\,\mathrm{nm}$. The latter is in accordance with the calculated value by (7). Furthermore, the use of this equation points to semiconducting chiral layer. It is possible to estimate whether the choice of these equations was justified by checking the accordance with $N = \dfrac{d_o - d_i}{2\delta_r} + 1$, when calculating the average interlayer distance δ_r in CNT_3. Using the values N=6, $d_o^{(3)} = 4.04\,\mathrm{nm}$, and $d_i^{(3)} = 0.65\,\mathrm{nm}$, thus obtaining $\delta_r = 0.339\,\mathrm{nm}$, is an excellent indicator that the diameters are well estimated. The innermost and the outermost diameters are out of the high accuracy diameter range 1-2.5 nm, and obtained by different equations. The possible (*m*,*n*) assignment was performed using Python programming, equation (2) and corresponding error bars.

For the outermost diameter, there were three possibilities in the interval $(d_o^{(3)} - 0.002,\, d_o^{(3)} + 0.002)$: (31,28), (32,27), and (49,4), each being chiral. However, considering the semiconducting nature of this layer, the only pair of chiral indices satisfying the condition $\mathrm{MOD}(2m+n,3) \neq 0$ is (32,27).

With regard to the innermost diameter, the possible (*m*,*n*) assignment was performed in the interval $(d_i^{(3)} - 0.02, d_i^{(3)} + 0.02)$ resulting into two possibilities: (7,2) and (8,0), of which it must be emphasized that the pair (7,2) is within a much lower error bar. Both of these possibilities point to a semiconducting layer.

There are two possible combinations: (7,2)@@(32,27) and (8,0)@@(32,27). The option (7,2)@@(32,27) was discussed to be within a smaller error bar, and also its calculated interlayer distance of 0.340 nm is closer to the determined $\delta_r = 0.339\,\text{nm}$, than the distance of 0.341 nm that holds for the option (8,0)@@(32,27). However, these findings are not enough of a discrepancy at the latter option in order to be excluded.

In Fig. 10 there is an illustration of the two candidates with determined diameters and chiral indices assignment to the tube CNT_3.

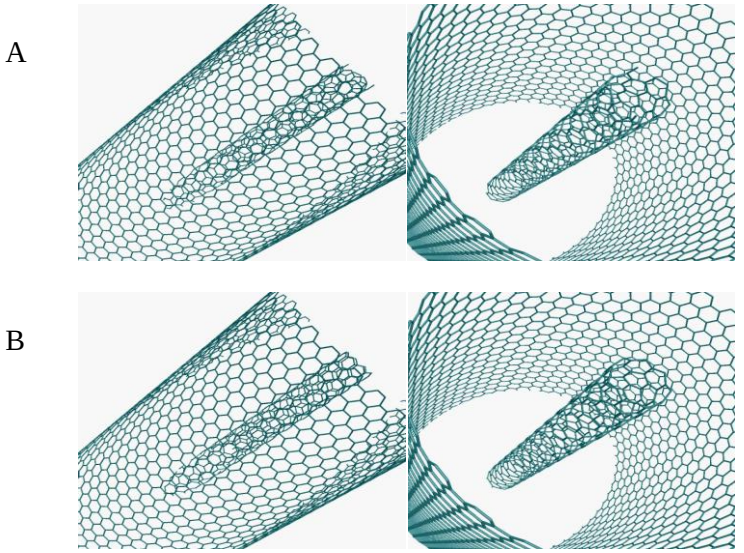

Figure 10: Visual model of A) (7,2)@@(32,27);
B) (8,0)@@(32,27)

Considering this nanotube CNT_3 it is again strongly suggested an additional EDP analysis to be performed. This would differentiate the two candidates, since they have different *m*/*n* ratios of the innermost constituent tubes, and hence it is highly expected that the EDP would leave only one possible candidate.

4. CONCLUSIONS

Based on the analysis aned discussions in previous sections, several important findings may be concluded:

- Determination of three CNTs atomic structure has been performed; fully for CNT_1 and CNT_2, and partially for CNT_3 (as presented in Table 4);
- The thorough analyses were made with regard to the CNTs' Raman spectra in RBLM and G-mode frequency regions, combined with use of Python programming;
- The performed calculations were in excellent agreement with the theoretical background and with control methods;
- The calculations can be further improved in terms of higher accuracy, and corresponding methods, as EDP, are strongly suggested;
- The results enable many applications, as well as providing full necessary information for graph theorists who work on topological indices.

Table 4: Summarized results to specify studied CNTs

Parameters in nanotube	**CNT_1**	**CNT_2**	**CNT_3**
Chiral indices (*m*,*n*)	(6,0)	(17,6)@(25,7) (19,3)@(25,7)	(7,2)@@(32,27) (8,0)@@(32,27)
Diameters (in nm)	0.665	1.63@2.3	0.65@4.04
Interlayer distances (in nm)	-	0.335	0.34
Number of walls	1	2	6
Conducting nature	MZ	SC@MC	SC@@SC (intrinsically Metallic)
Chiral angles (in rad)	0	0.25@0.21 0.13@0.21	0.21@@0.47 0@@0.47
Length of the unit cell (in nm)	0.6	8.87@4.17 8.87@4.17	3.54@@21.98 0.44@@21.98
Number of hexagons in the UC	12	854@566 854@566	134@5234 16@5234

COMPETING INTERESTS

Authors have declared that no competing interests exist.

ACKNOWLEDGMENTS

This study was done within the following EU projects: COST Action CA17139 “European Topology Interdisciplinary Action”, and COST Action CA17140 “Cancer nanomedicine - from the bench to the bedside”.

References

[1] M.S. Dresselhaus, G. Dresselhaus, R. Saito, A. Jorio, *Raman spectroscopy of carbon nanotubes*, Physics Reports 409 (2005), 47–99.
[2] X. Zhao, Y. Ando, L.-C. Qin, H. Kataura, Y. Maniwa, R. Saito, *Radial breathing modes of multiwalled carbon nanotubes*, Chem. Phys. Lett. 361 (2002), 169–174.
[3] C. Schwandt, A.T. Dimitrov, D.J. Fray, *High-yield synthesis of multi-walled carbon nanotubes from graphite by molten salt electrolysis*, Carbon 50 (2012), 1311–1315.
[4] B. Andonovic, A. Ademi, A. Grozdanov, P. Paunović, Aleksandar T. Dimitrov, *Enhanced model for determining the number of graphene layers and their distribution from X-ray diffraction data*, Beilstein J. Nanotechnol 6 (2015), 2113-2122.
[5] D.I. Levshov, H.N. Tran, M. Paillet, R. Arenal, X.T. Than, A.A. Zahab, Y.I. Yuzyuk, J.-L. Sauvajol, T. Michel, *Accurate determination of the chiral indices of individual carbon nanotubes by combining electron diffraction and Resonant Raman spectroscopy*, Carbon 114 (2017), 141-159.
[6] T. Natsuki, G.J.H. Melvin & Q.-Q. Ni. *Vibrational Frequencies and Raman Radial Breathing Modes of Multi-Walled Carbon Nanotubes Based on Continuum Mechanics*, Journal of Materials Science Research 2, (4) (2013).
[7] J.M. Benoit, J.P. Buisson, O. Chauvet, C. Godon, and S. Lefrant. *Low-frequency Raman studies of multiwalled carbon nanotubes: Experiments and theory*, Phys. Rev. B, 66 (7) (2002), 073417.
[8] B. Andonovic, V. Andova, T. Atanasova Pacemska, P. Paunovic, V. Andonovic, J. Djordjevic, & A. Dimitrov, *Distance based topological indices on multiwall carbon nanotubes samples obtained by electrolysis in molten salts*. BJAMI, 3(1), (2020), 7-12.
[9] O.V. Kharissova, B.I. Kharisov, *Variations of interlayer spacing in carbon nanotubes*, RSC Adv., 4, (2014), 30807-30815
[10] L. Qin, X. Zhao, K. Hirahara, et al, The smallest carbon nanotube, Nature 408, 50, (2000), 50-51.

Jožef Stefan Institute, Ljubljana, Slovenia
E-mail address: viktor.andonovikj@ijs.si
Faculty of Technology and Metallurgy, University “St Cyril and Methodius”, Skopje, Macedonia
E-mail address: aco@tmf.ukim.edu.mk
Faculty of Technology and Metallurgy, University “St Cyril and Methodius”, Skopje, Macedonia
E-mail address: pericap@tmf.ukim.edu.mk
Faculty of Technology and Metallurgy, University “St Cyril and Methodius”, Skopje, Macedonia
E-mail address: beti@tmf.ukim.edu.mk

Publisher
Union od Mathematicians of Macedonia – ARMAGANKA

Editor in chief
Prof. d-r Aleksa Malcheski

CIP - Каталогизација во публикација
Национална и универзитетска библиотека "Св. Климент Охридски", Скопје

51(082)

PROCEEDINGS of CODEMA 2020 = Зборник на трудови од CODEMA 2020. -
Skopje : Armaganka, 2021. - 375 стр. : илустр. ; 25 см

Текст на мак. и англ. јазик. - Фусноти кон текстот. - Библиографија кон трудовите

ISBN 978-608-4904-09-0

а) Математика -- Зборници

COBISS.MK-ID 53570309